

1 **Title: Rapid reconstruction of SARS-CoV-2 using a synthetic genomics platform**

2 Short title: In yeast genome engineering of RNA viruses

3 Tran Thi Nhu Thao^{¶, 1,2,3}, Fabien Labroussaa^{¶, 2,4}, Nadine Ebert^{¶, 1,2}, Philip V'kovski^{1,2},
4 Hanspeter Stalder^{1,2}, Jasmine Portmann^{1,2}, Jenna Kelly^{1,2}, Silvio Steiner^{1,2,3}, Melle
5 Holwerda^{1,2,3,5}, Annika Kratzel^{1,2,3}, Mitra Gultom^{1,2,3,5}, Laura Laloli^{1,2,3,5}, Linda Hüsser^{1,2},
6 Manon Wider⁵, Stephanie Pfaender^{1,2}, Dagny Hirt^{1,2}, Valentina Cippà^{2,4}, Silvia Crespo-
7 Pomar^{2,4}, Simon Schröder⁶, Doreen Muth^{6,7}, Daniela Niemeyer^{6,7}, Marcel A. Müller^{6,7,8},
8 Christian Drosten^{6,7}, Ronald Dijkman^{1,2,5}, Joerg Jores^{§,*, 2,4}, Volker Thiel^{§,*, 1,2}

9 ¹*Institute of Virology and Immunology (IVI), Bern, Switzerland*

10 ²*Department of Infectious Diseases and Pathobiology, Vetsuisse Faculty, University of Bern,*
11 *Bern, Switzerland*

12 ³*Graduate School for Biomedical Science, University of Bern, Bern, Switzerland*

13 ⁴*Institute of Veterinary Bacteriology, Vetsuisse Faculty, University of Bern, Bern, Switzerland*

14 ⁵*Institute for Infectious Diseases, University of Bern, Bern, Switzerland*

15 ⁶*Institute of Virology, Charité-Universitätsmedizin Berlin, corporate member of Freie*
16 *Universität Berlin, Humboldt-Universität zu Berlin, and Berlin Institute of Health, Berlin,*
17 *Germany*

18 ⁷*German Centre for Infection Research, associated partner Charité, Berlin, Germany.*

19 ⁸*Martsinovskiy Institute of Medical Parasitology, Tropical and Vector Borne Diseases,*
20 *Sechenov University, Moscow, Russia.*

21

22 ^{¶, §}: *equally contributed*

23 **corresponding authors:*

24 *Volker Thiel; e-mail: volker.thiel@vetsuisse.unibe.ch; phone: +41-31-6312413*

25 *Joerg Jores; e-mail: joerg.jores@vetsuisse.unibe.ch; phone: +41-31-6312414*

26 Abstract : 207 words ; main text : 2373 words.

27 **Abstract**

28 Reverse genetics has been an indispensable tool revolutionising our insights into viral
29 pathogenesis and vaccine development. Large RNA virus genomes, such as from
30 Coronaviruses, are cumbersome to clone and to manipulate in *E. coli* hosts due to size and
31 occasional instability¹⁻³. Therefore, an alternative rapid and robust reverse genetics platform
32 for RNA viruses would benefit the research community. Here we show the full functionality
33 of a yeast-based synthetic genomics platform for the genetic reconstruction of diverse RNA
34 viruses, including members of the *Coronaviridae*, *Flaviviridae* and *Paramyxoviridae* families.
35 Viral subgenomic fragments were generated using viral isolates, cloned viral DNA, clinical
36 samples, or synthetic DNA, and reassembled in one step in *Saccharomyces cerevisiae* using
37 transformation associated recombination (TAR) cloning to maintain the genome as a yeast
38 artificial chromosome (YAC). T7-RNA polymerase has been used to generate infectious
39 RNA, which was then used to rescue viable virus. Based on this platform we have been able
40 to engineer and resurrect chemically-synthesized clones of the recent epidemic SARS-CoV-2⁴
41 in only a week after receipt of the synthetic DNA fragments. The technical advance we
42 describe here allows to rapidly responding to emerging viruses as it enables the generation
43 and functional characterization of evolving RNA virus variants - in real-time - during an
44 outbreak.

45 **Main Text**

46 Population growth, increased travel and climate change foster epidemic and pandemic threats
47 by (re)emerging RNA viruses. Although black swan events cannot be predicted, our medical
48 sector should be ready to use the latest advancements in science to combat emerging viruses.
49 Within the past decade we have seen outbreaks of Middle-East Respiratory Syndrome
50 coronavirus (MERS-CoV)⁵, ZIKA virus (ZIKV)⁶, Ebola virus⁷, and at the end of 2019,
51 SARS-CoV-2 that was first detected in Wuhan, Hubei province, China⁴, but meanwhile
52 spread throughout China and beyond. Until now SARS-CoV-2 isolates from China have not
53 been shared with health authorities and the scientific community, although they are urgently
54 needed to build up serological diagnostics, to develop and assess antivirals and vaccines, and
55 to establish appropriate *in vivo* models. Generation of SARS-CoV-2 from chemically
56 synthesized DNA could bypass the limited availability of virus isolates and would
57 furthermore allow genetic modifications and functional characterization of individual genes.
58 However, although the workhorse *E. coli* did prove very useful for cloning many viral
59 genomes, it has drawbacks for a number of emerging RNA viruses, including coronaviruses,
60 in terms of assembling and stably maintaining full-length molecular clones.

61 Synthetic genomics is a field that was fuelled by the efforts to create a bacterial cell that is
62 controlled by a synthetic genome⁸. Genome-wide reassembly of the ~1.1Mb *Mycoplasma*
63 genome was first attempted using *E. coli* as an intermediate host⁸, but the maintenance of
64 these 100-kbp DNA fragments appeared to be very difficult in this host. Therefore, the yeast
65 *Saccharomyces cerevisiae* was chosen to clone, assemble and even mutagenize entire
66 *Mycoplasma* genomes^{9,10}. This ultimately led to the construction of the Mycoplasma JCVI
67 Syn3.0, a cell carrying the minimal set of genes allowing its autonomous replication in
68 auxotrophic medium¹¹. The rationale for using a yeast cloning system is the ability of yeast to

69 recombine overlapping DNA fragments *in cellulo*, which led to the development of a
70 technique called “transformation-associated recombination” (TAR) cloning¹².

71 More recently, TAR cloning was successfully applied for the assembly, genetic engineering
72 and rescue of large DNA viruses such as cytomegalovirus and herpes simplex virus 1^{13,14}.

73 While large DNA viruses such as herpesviruses can be rescued by transfecting the entire viral
74 DNA genome into eukaryotic cells, the rescue of RNA viruses requires the transcription of a
75 viral genomic RNA from the cloned DNA template. For coronaviruses that belong to a family
76 of positive-stranded RNA viruses termed *Coronaviridae*, the generation of full-length
77 molecular clones has long been hampered by the extraordinary genome size (27-31 kb) and
78 occasional instability of cloned DNA in *E. coli*. It took until 2000/2001 before unconventional
79 approaches, such as cloning in low copy bacterial artificial chromosomes (BACs) or vaccinia
80 virus, or cloning of subgenomic DNA fragments followed by *in-vitro* ligation, were
81 successful¹⁻³. However, each system has caveats leaving the generation of recombinant
82 coronaviruses cumbersome. We therefore aimed to assess the use of the yeast *S. cerevisiae* to
83 assemble and maintain genomes of diverse RNA viruses in order to establish a rapid, stable,
84 and universal reverse genetics pipeline for RNA viruses.

85 In an effort to adopt a yeast-based reverse genetics platform to RNA viruses we first tested the
86 Murine hepatitis virus strain A59 containing the gene for the green fluorescent protein (MHV-
87 GFP), which is routinely used in our laboratory and has an established vaccinia virus-based
88 reverse genetics platform^{15,16}. The overall strategy is shown in Fig. 1a. Viral RNA was
89 prepared from MHV-GFP-infected murine 17Cl-1 cells and used to amplify 7 overlapping
90 DNA fragments by RT-PCR together spanning the MHV-GFP genome from nt 2024 to nt
91 29672. Fragments containing the 5'- and 3'-termini were PCR-amplified from the vaccinia
92 virus-cloned genome to include a T7-RNA polymerase promoter and a cleavage site (*PacI*)
93 following the polyA sequence. Overlaps to the TAR vector pVC604 were included in the

94 primers used to amplify the 5'- and 3'-terminal fragments and the pVC604 backbone that was
95 also generated by PCR (Fig. 1b, Table 1, Extended Data Table 1, Extended Data Figure 1a).
96 All DNA fragments were used to transform *Saccharomyces cerevisiae* (strain VL6-48N) and
97 resulting colonies were screened for correct assembly of the YAC containing the MHV
98 genome by multiplex PCRs that covered the junctions of the different fragments. This screen
99 revealed that > 90 % of the clones tested were positive indicating a highly efficient assembly
100 in yeast (Extended Data Figure 1a). To rescue MHV-GFP we randomly chose two clones,
101 purified the YAC, linearized the plasmid using the restriction endonuclease *PacI* (Extended
102 Data Table 2) and subjected it to T7 RNA polymerase-based *in vitro* transcription to generate
103 capped viral genomic RNA. This RNA was transfected together with an *in vitro* transcribed
104 mRNA encoding the MHV nucleocapsid (N) protein into BHK-MHV-N cells as previously
105 described¹⁵. Transfected BHK-MHV-N cells were mixed with MHV-susceptible 17Cl-1 cells
106 and cytopathic effect (CPE), virus-induced syncytia, and GFP-expressing cells were readily
107 detectable for both clones within 48 hours, indicating successful recovery of infectious virus
108 (Fig. 1c). Finally, we assessed the replication kinetics of the recovered viruses, which were
109 indistinguishable compared to the parental MHV-GFP (Fig. 1d).

110 To address if the synthetic genomics platform can be applied to other coronaviruses, and if it
111 can be used for rapid mutagenesis, we used a molecular BAC clone of MERS-CoV¹⁷. We
112 PCR-amplified eight subgenomic overlapping DNA fragments covering the entire MERS-
113 CoV genome (Figure 2a, Extended Data Figure 1b, Extended Data Table 1). The 5'- and 3'-
114 terminal DNA fragments contained the T7-RNA polymerase promoter upstream the MERS-
115 CoV 5'-end and a restriction endonuclease cleavage site *MluI* downstream the polyA
116 sequence, and overlapping sequences with the TAR plasmid pVC604. To mutagenize the
117 MERS-CoV clone and introduce the GFP gene, fragment 7 was modified to overlap with the
118 PCR-amplified GFP gene. Following transformation almost all YAC clones were positive for
119 the junctions indicating a successful assembly (Figure 2a, Extended Data Figure 1b). Virus

120 rescue from cloned DNA was performed as described previously¹⁷ and virus-induced CPE
121 became apparent in VeroB4 cells inoculated with recovered recombinant MERS-CoV (Fig.
122 2b). Importantly, we could readily detect green fluorescent VeroB4 cells that had been
123 infected with recovered MERS-CoV-GFP demonstrating that the synthetic genomics platform
124 is suitable to genetically modify coronavirus genomes (Fig. 2b). As expected replication
125 kinetics of recombinant MERS-CoV and MERS-CoV-GFP were slightly reduced compared to
126 cell-culture-adapted MERS-CoV-EMC (Fig. 2c).

127 Having shown that the TAR cloning approach is robust and reproducible, we aimed to
128 thoroughly evaluate the system concerning stability of cloned sequences, the range of
129 applicability to other virus genomes, and if molecular clones can even be generated from
130 clinical samples. The yeast clones containing YACs encoding MHV-GFP and MERS-CoV
131 were passaged 15-17 times followed by re-sequencing. Results of this experiment were very
132 supportive of the yeast-based platform (Extended Data Table 3), since the genomes could be
133 stably maintained and no mutations arose. We then embarked on cloning a number of other
134 coronaviruses (HCoV-229E², HCoV-HKU1; GenBank: NC_006577, MERS-CoV-Riyadh-
135 1734-2015; GenBank: MN481979) and viruses of other families, such as ZIKV (family
136 *Flaviviridae*, GenBank: KX377337) and human respiratory-syncytial-virus (hRSV; family
137 *Paramyxoviridae*) (Table 1) that are known to be difficult to clone and stably maintain in *E.*
138 *coli*. As shown in Extended data Figure 1d-h, we followed the same strategy to prepare the
139 genome termini in cloned plasmids to include genetic elements that are later needed for virus
140 rescue (e.g. T7-RNA polymerase promoter, cleavages sites or ribozyme elements) and
141 produced a set of overlapping DNA fragments covering the rest of the genome. This strategy
142 proved to be successful irrespectively of the source of virus or nucleic acid template or the
143 number of DNA fragments that were used for the one-step assembly in yeast. Of note, we
144 were also able to clone hRSV-B, without any prior information on the virus genotype, directly
145 from a clinical sample (nasopharyngeal aspirate) by designing RSV consensus primers to

146 amplify 4 overlapping DNA fragments (sequence submitted to GenBank). Collectively, these
147 results demonstrate the synthetic genomics platform provides the technical advance to rapidly
148 generate molecular clones of diverse RNA viruses by using viral isolates, cloned DNA,
149 synthetic DNA, and even clinical samples as starting material.

150 The appearance of a novel CoV in China at the end of 2019 prompted us to go a step further
151 and to test the applicability of our synthetic genomics platform to reconstruct the virus based
152 on its released genome sequence and chemically synthesized DNA fragments. Notably, at the
153 time when the first genome sequences of SARS-CoV-2 were released (Jan 10/11th, 2020) no
154 virus isolate has been made available and it took until the end of January 2020 when
155 successful isolation of SARS-CoV-2 was reported from patients in Australia
156 ([https://www.the-scientist.com/news-opinion/australian-lab-cultures-new-coronavirus-as-](https://www.the-scientist.com/news-opinion/australian-lab-cultures-new-coronavirus-as-infections-climb-67031)
157 [infections-climb-67031](https://www.the-scientist.com/news-opinion/australian-lab-cultures-new-coronavirus-as-infections-climb-67031)). We fragmented the genome into 12 subgenomic DNA fragments
158 ranging in size between 0.5-3.4 kbp (Fig. 3a, Extended Data Figure 1i, Extended Data Tables
159 1, 4). In parallel, we also aimed to generate a SARS-CoV-2 expressing GFP that could be
160 valuable to facilitate the establishment of serological diagnostics (e.g. virus neutralization
161 assay) and detection in cell culture. To do this we divided fragment 11 into 3 sub-fragments
162 (Fig. 3a, Extended Data Figure 1i, Extended Data Tables 1, 4) to include the GFP sequence,
163 which was inserted in frame within the ORF7a. We noticed at the 5' end of the reported
164 SARS-CoV-2 sequence that nucleotides 3-5 (5'-AUUAAAGG; Genbank MN996528.1) were
165 different compared to the closely related SARS-CoV (5'-AUAUUAGG; GenBank
166 AY291315) and to the even more closely related bat SARS-related CoVs ZXC21 and ZC45
167 (5'-AUAUUAGG)¹⁸, and that for all three the 5'-end has been experimentally determined by
168 5'-RACE^{4,18,19}. Therefore, we designed three 5'-end versions of fragment 1 containing the
169 reported SARS-CoV-2 sequence (fragment 1.3; 5'-AUUAAAGG), a version modified by 3
170 nucleotides (fragment 1.1; 5'-AUAUUAGG), and a version containing the 124 5'-terminal
171 nucleotides spanning the first four 5'-terminal stem-loop structures of SARS-CoV (fragment

172 1.2; Fig. 3b). Notably, nucleotide differences between SARS-CoV-2 and SARS-CoV within
173 this region are in agreement with the predicted RNA secondary structures (Fig. 3b).

174 We ordered the synthetic DNA constructs on January 14th (Fig. 3d, Extended data Table 4,
175 Extended Data Document 1), and until February 4th 12 of 14 constructs were delivered as
176 sequence-confirmed plasmids. However, fragments 5 and 7 turned out to be problematic to
177 clone in *E. coli* and could not be delivered. Since we received at the same time SARS-CoV-2
178 viral RNA obtained from an isolate of a Munich patient (SARS-CoV-2/München-
179 1.1/2020/929), we decided to amplify the regions of fragments 5 and 7 by RT-PCR. TAR
180 cloning was immediately initiated, and for all 6 SARS-CoV-2 constructs we obtained
181 correctly assembled molecular clones (3 versions of the 5'-end and each version with and
182 without GFP; Extended Data Fig. 2). Since sequence verification was not possible within this
183 short time frame, we randomly selected two clones for each construct for rescuing
184 recombinant rSARS-CoV-2 and rSARS-CoV-2-GFP. YAC DNA were isolated, *in vitro*
185 transcribed and the resulting RNAs electroporated together with an mRNA encoding the
186 SARS-CoV-2 N protein into BHK-21 and, in parallel, into BHK-SARS-N cells expressing the
187 SARS-CoV N protein²⁰. The BHK-21 and BHK-SARS-N cells were seeded over VeroE6
188 cells and at two days post electroporation we observed green fluorescent signals in cells that
189 received the GFP-encoding SARS-CoV-2 RNAs. Indeed supernatants transferred to fresh
190 VeroE6 cells contained infectious recombinant viruses for almost all recombinant rSARS-
191 CoV-2 and rSARS-CoV-GFP constructs (Extended Data Fig. 2). As shown in Figure 3c for
192 SARS-CoV-2 clones 1.1, 2.2, and 3.1, plaques were detectable on VeroE6 cells that were
193 inoculated with supernatants containing the RNA-electroporated cells, demonstrating the
194 infectious virus has been recovered for recombinant rSARS-CoV-2 and for the variants
195 containing modified 5'-termini. Similarly, we could detect green fluorescent cells on VeroE6
196 monolayers that were inoculated with supernatants from RNA-electroporated cells of rSARS-
197 CoV-2-GFP clones 4.1, 5.2 and 6.1, demonstrating that recombinant GFP-expressing viruses

198 have been recovered for all 5'-end variants. This result demonstrates the full functionality of
199 the SARS-CoV-2 reverse genetics system and also shows that the 5'-ends of SARS-CoV and
200 bat SARS-related CoVs ZXC21 and ZC45 are compatible with the replication machinery of
201 SARS-CoV-2.

202 We expect that the fast, robust and versatile synthetic genomics platform we describe here
203 will provide new insights into the molecular biology and pathogenesis of a number of
204 emerging RNA viruses and will specifically facilitate the molecular characterization of the
205 novel coronavirus SARS-CoV-2. Although homologous recombination in yeast has already
206 been used for the generation of a number of molecular virus clones in the past^{13,14,21}, we
207 present here a thorough evaluation of the feasibility of this approach to rapidly generate full-
208 length cDNAs for large RNA viruses that have a known history of instability in *E. coli*. We
209 show that one main advantage of the TAR cloning system is that the viral genomes can be
210 fragmented to at least 14 overlapping fragments and re-assembled with remarkable efficacy
211 (usually >90% of the clones are correct). This allowed us to complete the cloning and rescue
212 of rSARS-CoV-2 and rSARS-CoV-2-GFP within one week. It should also be noted that we
213 see considerable potential to reduce the time of DNA synthesis. Currently, synthetic DNA
214 fragments are still routinely cloned in *E. coli*, which turned out to be problematic for SARS-
215 CoV-2 fragments 5 and 7. We could however use 4 and 3 shorter dsDNA parts of fragments 5
216 and 7, respectively, that we received, to assemble the full-length fragments 5 and 7 by TAR
217 cloning which is an additional proof of the superior cloning efficiency of our yeast system
218 versus *E. coli*-based systems. This allowed us to generate a molecular clone of SARS-CoV-2
219 by using exclusively chemically synthesized DNA, and the rescue of this version is currently
220 in progress.

221 The appearance of SARS-CoV-2 emphasizes the need for preparedness to rapidly respond to
222 emerging virus threats. While the availability of SARS-CoV-2 isolates is still limited, full

223 virus genome sequences were disclosed very early during the outbreak. The rapidity of our
224 synthetic genomics approach to generate SARS-CoV-2 and the applicability to other
225 emerging RNA viruses make this system an attractive alternative to provide infectious virus
226 to health authorities and diagnostic laboratories without the need to have access to clinical
227 samples. Finally, as the SARS-CoV-2 outbreak is ongoing, we expect to see sequence
228 variations and possibly phenotypic changes of evolving SARS-CoV-2 in the human host.
229 With the synthetic genomics platform it is now possible to introduce such sequence variations
230 into the infectious clone and to functionally characterize SARS-CoV-2 evolution in real-time.

231

232

233 **References**

- 234 1 Almazan, F. *et al.* Engineering the largest RNA virus genome as an infectious
235 bacterial artificial chromosome. *Proc Natl Acad Sci U S A* **97**, 5516-5521,
236 doi:10.1073/pnas.97.10.5516 (2000).
- 237 2 Thiel, V., Herold, J., Schelle, B. & Siddell, S. G. Infectious RNA transcribed in vitro
238 from a cDNA copy of the human coronavirus genome cloned in vaccinia virus. *J Gen
239 Virol* **82**, 1273–1281 (2001).
- 240 3 Yount, B., Curtis, K. M. & Baric, R. S. Strategy for systematic assembly of large RNA
241 and DNA genomes: transmissible gastroenteritis virus model. *J Virol* **74**, 10600-
242 10611, doi:10.1128/jvi.74.22.10600-10611.2000 (2000).
- 243 4 Zhu, N. *et al.* A Novel Coronavirus from Patients with Pneumonia in China, 2019. *N
244 Engl J Med*, doi:10.1056/NEJMoa2001017 (2020).
- 245 5 Zaki, A. M., van Boheemen, S., Bestebroer, T. M., Osterhaus, A. D. & Fouchier, R. A.
246 Isolation of a novel coronavirus from a man with pneumonia in Saudi Arabia. *N Engl
247 J Med* **367**, 1814-1820, doi:10.1056/NEJMoa1211721 (2012).
- 248 6 Cao-Lormeau, V. M. *et al.* Zika virus, French polynesia, South pacific, 2013. *Emerg
249 Infect Dis* **20**, 1085-1086, doi:10.3201/eid2006.140138 (2014).
- 250 7 Baize, S. *et al.* Emergence of Zaire Ebola virus disease in Guinea. *N Engl J Med* **371**,
251 1418-1425, doi:10.1056/NEJMoa1404505 (2014).
- 252 8 Gibson, D. G. *et al.* Creation of a Bacterial Cell Controlled by a Chemically
253 Synthesized Genome. *Science* **329**, 52-56, doi:science.1190719 [pii]
254 10.1126/science.1190719 (2010).
- 255 9 Lartigue, C. *et al.* Creating bacterial strains from genomes that have been cloned and
256 engineered in yeast. *Science* **325**, 1693-1696, doi:1173759 [pii]
257 10.1126/science.1173759 (2009).

- 258 10 Benders, G. A. *et al.* Cloning whole bacterial genomes in yeast. *Nucleic Acids Res* **38**,
259 2558-2569, doi:10.1093/nar/gkq119 (2010).
- 260 11 Hutchison, C. A., 3rd *et al.* Design and synthesis of a minimal bacterial genome.
261 *Science* **351**, aad6253, doi:10.1126/science.aad6253 (2016).
- 262 12 Kouprina, N. & Larionov, V. Selective isolation of genomic loci from complex
263 genomes by transformation-associated recombination cloning in the yeast
264 *Saccharomyces cerevisiae*. *Nat Protoc* **3**, 371-377, doi:10.1038/nprot.2008.5 (2008).
- 265 13 Vashee, S. *et al.* Cloning, Assembly, and Modification of the Primary Human
266 Cytomegalovirus Isolate Toledo by Yeast-Based Transformation-Associated
267 Recombination. *mSphere* **2**, doi:10.1128/mSphereDirect.00331-17 (2017).
- 268 14 Oldfield, L. M. *et al.* Genome-wide engineering of an infectious clone of herpes
269 simplex virus type 1 using synthetic genomics assembly methods. *Proc Natl Acad Sci*
270 *U S A* **114**, E8885-E8894, doi:10.1073/pnas.1700534114 (2017).
- 271 15 Coley, S. E. *et al.* Recombinant mouse hepatitis virus strain A59 from cloned, full-
272 length cDNA replicates to high titers in vitro and is fully pathogenic in vivo. *J Virol*
273 **79**, 3097-3106, doi:10.1128/JVI.79.5.3097-3106.2005 (2005).
- 274 16 Zust, R. *et al.* Coronavirus non-structural protein 1 is a major pathogenicity factor:
275 implications for the rational design of coronavirus vaccines. *PLoS Pathog* **3**, e109,
276 doi:10.1371/journal.ppat.0030109 (2007).
- 277 17 Muth, D. *et al.* Transgene expression in the genome of Middle East respiratory
278 syndrome coronavirus based on a novel reverse genetics system utilizing Red-
279 mediated recombination cloning. *J Gen Virol* **98**, 2461-2469,
280 doi:10.1099/jgv.0.000919 (2017).
- 281 18 Hu, D. *et al.* Genomic characterization and infectivity of a novel SARS-like
282 coronavirus in Chinese bats. *Emerg Microbes Infect* **7**, 154, doi:10.1038/s41426-018-
283 0155-5 (2018).

- 284 19 Thiel, V. *et al.* Mechanisms and enzymes involved in SARS coronavirus genome
285 expression. *J Gen Virol* **84**, 2305-2315, doi:10.1099/vir.0.19424-0 (2003).
- 286 20 van den Worm, S. H. *et al.* Reverse genetics of SARS-related coronavirus using
287 vaccinia virus-based recombination. *PLoS One* **7**, e32857,
288 doi:10.1371/journal.pone.0032857 (2012).
- 289 21 Polo, S., Ketner, G., Levis, R. & Falgout, B. Infectious RNA transcripts from full-
290 length dengue virus type 2 cDNA clones made in yeast. *J Virol* **71**, 5366-5374 (1997).
- 291 22 Chan, J. F. *et al.* Genomic characterization of the 2019 novel human-pathogenic
292 coronavirus isolated from a patient with atypical pneumonia after visiting Wuhan.
293 *Emerg Microbes Infect* **9**, 221-236, doi:10.1080/22221751.2020.1719902 (2020).
- 294

295 Acknowledgements

296 This work was supported by the European Commission (Marie Skłodowska-Curie Innovative
297 Training Network “HONOURS”; grant agreement No 721367), the Swiss National Science
298 Foundation (SNF; grants CRSII3_160780, and 310030_173085), the German Research
299 Council (DFG; grants SFB-TR84 (TRR 84/3, A07), and DR 772/7-2), the Federal Ministry of
300 Education and Research (BMBF; grant RAPID, #01KI1723A) and by core funds of the
301 University of Bern. We thank the J. Craig Venter Institute (JCVI) for provision of the TAR
302 vectors. We thank specifically Eric Sun and Tibbers Zhang and are grateful for the timely
303 provision of the synthetic DNA fragments from GenScript. We thank Jeanne Peters Zocher
304 from VETCOM Zürich for her advice in generating the figures and we thank Franziska Suter-
305 Riniker and Pascal Bittel, Institute for Infectious Diseases, University of Bern, for providing
306 clinical samples. We thank Philippe Plattet, Markus Gerber, Martina Friesland, Marco Alves,
307 Nathalie Vielle, Beatrice Zumkehr, Melanie Brügger, Daniel Brechbühl for reagents,
308 technical advise and helpful discussions.

309 Authors contributions

310 VT and JJ conceived the study. TT, NE and FL performed most of the experiments. PV, HS,
311 JP, SSt, MH, AK, MG, LL, LH, MW, SP, DH, VC, SC, SSch, DM, DN, MM, CD, RD, did
312 experimental work and/or provided essential experimental systems and reagents. TT, NE, FL,
313 HS, JK, and RD performed sequencing including computational analyses. VT, JJ, TT, FL, NE
314 wrote the manuscript and made the figures. All authors read and approved the final
315 manuscript.

316 Ethical statement

317 The authors are aware that this work contains aspects of Dual Use Research of Concern
318 (DURC). The benefits were carefully balanced against the risks and the benefits outweigh the
319 risks. Permission to generate and work with recombinant SARS-CoV-2 and SARS-CoV-2-

320 GFP was granted by the Swiss Federal Office of Public Health (#A131191/3) with
321 consultation of the Federal Office for Environment, Federal Food Safety and Veterinary
322 Office, and the Swiss Expert Committee for Biosafety.

323 [Competing interests](#)

324 The authors declare no competing interests

325 [Additional information](#)

326 Correspondence and requests for material should be addressed to V.T. or J.J.

327 **Figure Legends**

328 **Figure 1. Application of yeast-based TAR cloning to generate viral cDNA clones and the**
329 **recovery of recombinant MHV-GFP.**

330 **a**, Schematic representation of the general workflow of TAR cloning and virus rescue. In-
331 yeast assembly require the delivery of overlapping DNA fragments covering the viral genome
332 and a TAR vector into yeast in one transformation event. Transformed DNA fragments are
333 joined by homologous recombination in yeast generating a YAC-cloned full-length viral
334 genomic cDNA. The *in vitro* production of infectious capped viral RNA starts with the
335 isolation of the YAC, followed by plasmid linearization to provide DNA template for run-off
336 T7 polymerase-based transcription. Virus rescue starts with electroporation of BHK-21 and/or
337 BHK-21 cells expressing the corresponding coronavirus N protein, followed by co-cultivation
338 of electroporated cells with susceptible cell line for virus production and amplification. **b**,
339 Schematic representation of MHV-GFP genome organisation with 9 viral subgenomic
340 overlapping cDNA fragments used for TAR cloning. pT7, T7 RNA polymerase promoter;
341 UTR, untranslated region; An, poly (A) tail; J represents assembly junction between two
342 overlapping DNA fragments. **c**, Recovery of infectious recombinant MHV-GFP. Cell culture
343 supernatants containing viruses produced after virus rescue from two MHV-GFP YAC clones
344 (Clone1, Clone 2) were used to infect 17Cl-1 cells. At 48 hours post-infection, infected cells
345 were visualised for GFP expression (left panels) and by bright field microscopy (right panels).
346 Mock represents 17Cl-1 cells inoculated with supernatant from BHK-MHV-N cells
347 electroporated without viral RNAs. **d**, Replication kinetics of parental MHV-GFP and
348 recombinant MHV-GFP Clone 1 and Clone 2. L929 cells were infected at an MOI of 0.1. Cell
349 culture supernatants were harvested at indicated time points post-infection and titrated by
350 plaque assay. Data are representative of three independent experiments with two replicates per

351 virus in each experiment. Error bars show standard deviation (SD) from the mean. pfu/ml,
352 plaque forming units per millilitre.

353

354 **Figure 2. Generation of viral cDNA clones and recovery of recombinant MERS-CoV**
355 **and MERS-CoV-GFP.**

356 **a**, Schematic representation of MERS-CoV (upper panel) and MERS-CoV-GFP (lower panel)
357 genome organization with 8 and 10 viral subgenomic overlapping cDNA fragments,
358 respectively, used for TAR cloning. pT7, T7 RNA polymerase promoter; UTR, untranslated
359 region; An, poly (A) tail; J represents assembly junction between two overlapping DNA
360 fragments. **b**, Rescue of recombinant MERS-CoV and MERS-CoV-GFP. Following delivery
361 of viral RNAs into BHK-21 cells via electroporation the cells were co-cultivated with VeroB4
362 cells and supernatants containing recombinant viruses produced were used to infect new
363 VeroB4 cells. Infected cells were visualised by bright field microscopy for recombinant
364 MERS-CoV (upper panel; 5 days post infection), and for GFP expression for recombinant
365 MERS-CoV-GFP (lower panel, 3 days post infection). Mock represents VeroB4 cells
366 inoculated with supernatant from BHK-21 cells electroporated without viral RNAs. **c**,
367 Replication kinetics of the MERS-CoV-EMC (laboratory adapted isolate), rMERS-CoV and
368 rMERS-CoV-GFP. VeroB4 cells were infected at an MOI of 0.01. Cell culture supernatants
369 were harvested at indicated time points post infection and titrated by TCID50 assay. Data are
370 representative of three independent experiments with two replicates per virus in each
371 experiment. Error bars show standard deviation (SD) from the mean. TCID50/ml, 50% tissue
372 culture infectious dose per millilitre.

373

374 **Figure 3. Generation of viral cDNA clones and recovery of recombinant SARS-CoV-2**
375 **and SARS-CoV-2-GFP. a**, Schematic representation of SARS-CoV-2 (upper panel) and

376 SARS-CoV-2-GFP (lower panel) genome organisation with 12 and 14 viral subgenomic
377 overlapping cDNA fragments, respectively, used for TAR cloning. pT7, T7 RNA polymerase
378 promoter; UTR, untranslated region; An, poly (A) tail; J represents assembly junction
379 between two overlapping DNA fragments. **b**, Representation of predicted RNA stem-loop
380 (SL) secondary structures formed in the 5'-UTR of SARS-CoV-2. The SARS-CoV-2 RNA
381 secondary structures were manually adjusted based on RNA structure predictions by Chan et
382 al.²². Black letters and numbering represents the SARS-CoV-2 5'-terminal sequence. Red
383 letters depict nucleotides that are different within the SARS-CoV 5'-terminal sequence (“-“
384 indicates nucleotide deletion in SARS-CoV versus SARS-CoV-2). N20 indicates 20
385 nucleotides. SL structures 1, 2, and 4 are shown according to Chan *et al.*²². Note that
386 recombinant virus construct 1 (rSARS-CoV-2 clone 1) and construct 4 (rSARS-CoV-GFP
387 clone 4) contain the SARS-CoV-2 5'-terminus with nucleotides 3-5 (UAA) exchanged by
388 nucleotides 3-5 (AUU) of SARS-CoV; recombinant virus construct 2 (rSARS-CoV-2 clone 2)
389 and construct 5 (rSARS-CoV-2-GFP clone 5) contain a 5'-terminus with the first 124
390 nucleotides from SARS-CoV; and recombinant virus construct 3 (rSARS-CoV-2 clone 3) and
391 construct 6 (rSARS-CoV-GFP clone 6) contain the authentic SARS-CoV-2 5'-terminus. **c**,
392 Rescue of recombinant rSARS-CoV-2 and rSARS-CoV-2-GFP. The experimental setting is
393 illustrated in the upper panel. Two clones of each construct 1-6 were used to prepare YAC
394 DNAs and *in-vitro* transcribed viral genome RNAs were electroporated into BHK-21 cells
395 and/or BHK-SARS-N together with an mRNA encoding the SARS-CoV-2 N protein.
396 Electroporated cells were co-cultivated with VeroE6 cells in a T25 flask and cell culture
397 supernatants were transferred to 12-well plates to perform plaque assay for rSARS-CoV-2
398 constructs 1-3 and fluorescence microscopy for rSARS-CoV-2-GFP constructs 4-6. Plaque
399 assays are shown in the lower panel for SARS-CoV-2 clones 1.1, 2.2, and 3.1. VeroE6 cells
400 were infected with 10^{-1} , 10^{-2} , and 10^{-3} dilutions of 1 ml supernatant from the individual rescue
401 experiments and are compared to non-infected cells (Mock). The expression of GFP in SARS-

402 CoV-2-GFP infected VeroE6 cells is shown for clones 4.1, 5.2, and 6.1. Mock represents non-
403 infected VeroE6 cells. **d**, Summary of the timeline of events of the SARS-CoV-2 outbreak
404 and the work leading to the reconstruction and recovery of rSARS-CoV-2.

405

406 **Extended Data Figure 1**

407 **a**, Schematic representation of the MHV-GFP genome organisation (upper panel) and nine
408 viral subgenomic cDNA fragments (F1-9) used for TAR cloning. Viral open reading frames
409 (ORFs), the ORF for GFP and sequence elements at the 5'- and 3'-untranslated regions
410 (UTRs) are indicated. Primers used to generate the fragments are listed in Extended Data
411 Table 1. J2-9 represent the junctions, i.e. overlapping regions, between the subgenomic cDNA
412 fragments. J1 and J10 represent junctions with the TAR vector. Gel images show results from
413 two multiplex PCRs that were designed to detect the presence of correctly recombined
414 junctions J1-10, confirming the proper assembly of the YAC containing the viral genome in
415 12 out of 12 clones. kb, kilobases; pT7, T7 RNA polymerase promoter; An, poly (A) tail.

416

417 **b**, Schematic representation of the MERS-CoV genome organisation (upper panel) and eight
418 viral subgenomic cDNA fragments (F1-8) used for TAR cloning. Viral open reading frames
419 (ORFs) and sequence elements at the 5'- and 3'-untranslated regions (UTRs) are indicated.
420 Primers used to generate the fragments are listed in Extended Data Table 1. J2-8 represent the
421 junctions, i.e. overlapping regions, between the subgenomic cDNA fragments. J1 and J9
422 represent junctions with the TAR vector. Gel image shows results from a multiplex PCR that
423 was designed to detect the presence of correctly recombined junctions J1-9, confirming the
424 proper assembly of the YAC containing the viral genome in 6 out of 8 clones. kb, kilobases;
425 pT7, T7 RNA polymerase promoter; An, poly (A) tail.

426

427 **c**, Schematic representation of the MERS-CoV-GFP genome organisation (upper panel) and
428 ten viral subgenomic cDNA fragments (F1-10 and F13) used for TAR cloning. Viral open
429 reading frames (ORFs), ORF for GFP and sequence elements at the 5'- and 3'-untranslated
430 regions (UTRs) are indicated. Primers used to generate the fragments are listed in Extended
431 Data Table 1. J2-8 and J10-11 represent the junctions, i.e. overlapping regions, between the
432 subgenomic cDNA fragments. J1 and J9 represent junctions with the TAR vector. Gel images
433 show results from two multiplex PCRs that were designed to detect the presence of correctly
434 recombined junctions J1-11, confirming the proper assembly of the YAC containing the viral
435 genome in 5 out of 8 clones. kb, kilobases; pT7, T7 RNA polymerase promoter; An, poly (A)
436 tail.

437

438 **d**, Schematic representation of the HCoV-229E genome organisation (upper panel) and
439 thirteen viral subgenomic cDNA fragments (F1-13) used for TAR cloning. Viral open reading
440 frames (ORFs) and sequence elements at the 5'- and 3'-untranslated regions (UTRs) are
441 indicated. Primers used to generate the fragments are listed in Extended Data Table 1. J2-13
442 represent the junctions, i.e. overlapping regions, between the subgenomic cDNA fragments.
443 J1 and J14 represent junctions with the TAR vector. Gel images show results from two
444 multiplex PCRs that were designed to detect the presence of correctly recombined junctions
445 J1-14, confirming the proper assembly of the YAC containing the viral genome in 7 out of 10
446 clones. kb, kilobases; pT7, T7 RNA polymerase promoter; An, poly (A) tail.

447

448 **d**, Schematic representation of the HCoV-HKU1 genome organisation (upper panel) and
449 eleven viral subgenomic cDNA fragments (F1-11) used for TAR cloning. Viral open reading
450 frames (ORFs) and sequence elements at the 5'- and 3'-untranslated regions (UTRs) are
451 indicated. Primers used to generate the fragments are listed in Extended Data Table 1. J2-11

452 represent the junctions, i.e. overlapping regions, between the subgenomic cDNA fragments.
453 J1 and J12 represent junctions with the TAR vector. Gel images show results from two
454 multiplex PCRs that were designed to detect the presence of correctly recombined junctions
455 J1-12, confirming the proper assembly of the YAC containing the viral genome in 14 out of
456 14 clones. kb, kilobases; pT7, T7 RNA polymerase promoter; An, poly (A) tail.

457 **e**, Schematic representation of the MERS-CoV-Riadh-1734-2015 genome organisation (upper
458 panel) and eight viral subgenomic cDNA fragments (F1-8) used for TAR cloning. Viral open
459 reading frames (ORFs) and sequence elements at the 5'- and 3'-untranslated regions (UTRs)
460 are indicated. Primers used to generate the fragments are listed in Extended Data Table 1. J2-8
461 represent the junctions, i.e. overlapping regions, between the subgenomic cDNA fragments.
462 J1 and J9 represent junctions with the TAR vector. Gel images show results from a multiplex
463 PCR and a simplex PCR, both of which were designed to detect the presence of correctly
464 recombined junctions J1-9, confirming the proper assembly of the YAC containing the viral
465 genome in 5 out of 8 clones. kb, kilobases; pT7, T7 RNA polymerase promoter; An, poly (A)
466 tail.

467

468 **f**, Schematic representation of the ZIKA virus genome organisation (upper panel) and six viral
469 subgenomic cDNA fragments (F1-6) used for TAR cloning. Viral open reading frames
470 (ORFs) and sequence elements at the 5'- and 3'-untranslated regions (UTRs) are indicated.
471 Primers used to generate the fragments are listed in Extended Data Table 1. J2-5 represent the
472 junctions, i.e. overlapping regions, between the subgenomic cDNA fragments. J1 and J6
473 represent junctions with the TAR vector. Gel image shows results from a multiplex PCR that
474 was designed to detect the presence of correctly recombined junctions J1-6, confirming the
475 proper assembly of the YAC containing the viral genome in 3 out of 15 clones. kb, kilobases;
476 pT7, T7 RNA polymerase promoter; HDR, hepatitis delta virus ribozyme.

477

478 **g**, Schematic representation of the human RSV-B virus genome organisation (upper panel)
479 and six viral subgenomic cDNA fragments (F1-6) used for TAR cloning. Viral open reading
480 frames (ORFs) and sequence elements at the 5'- and 3'-untranslated regions (UTRs) are
481 indicated. Primers used to generate the fragments are listed in Extended Data Table 1. J1-5
482 represent the junctions, i.e. overlapping regions, between the subgenomic cDNA fragments.
483 J1 and J5 contain junctions with the TAR vector. Gel image shows results from a multiplex
484 PCR that was designed to detect the presence of correctly recombined junctions J1-5,
485 confirming the proper assembly of the YAC containing the viral genome in 7 out of 8 clones.
486 kb, kilobases; pT7, T7 RNA polymerase promoter; HHrb, hammerhead ribozyme, Rb-T7ter,
487 Ribozyme and T7 RNA polymerase terminator sequence.

488

489 **h**, Schematic representation of the SARS-CoV-2 genome organisation (upper panel) and
490 twelve viral subgenomic cDNA fragments (F1-12) used for TAR cloning. Viral open reading
491 frames (ORFs) and sequence elements at the 5'- and 3'-untranslated regions (UTRs) are
492 indicated. Primers used to generate the fragments are listed in Extended Data Table 1. J2-12
493 represent the junctions, i.e. overlapping regions, between the subgenomic cDNA fragments.
494 J1 and J13 represent junctions with the TAR vector. Gel images show results from two
495 multiplex PCRs that were designed to detect the presence of correctly recombined junctions
496 J1-13, confirming the proper assembly of the YAC containing the viral genome in 6 out of 6
497 clones. kb, kilobases; pT7, T7 RNA polymerase promoter; An, poly (A) tail.

498

499 **i**, Schematic representation of the SARS-CoV-2 genome organisation (upper panel) and
500 fourteen viral subgenomic cDNA fragments (F1-10 and F12-15) used for TAR cloning. Viral
501 open reading frames (ORFs), ORF for GFP and sequence elements at the 5'- and 3'-

502 untranslated regions (UTRs) are indicated. Primers used to generate the fragments are listed in
503 Extended Data Table 1. J2-12 and J14 represent the junctions, i.e. overlapping regions,
504 between the subgenomic cDNA fragments. J1 and J13 represent junctions with the TAR
505 vector. Gel images show results from two multiplex PCRs and a simplex PCR, all of which
506 were designed to detect the presence of correctly recombined junctions J1-13 and J14
507 respectively, confirming the proper assembly of the YAC containing the viral genome in 6 out
508 of 6 clones. kb, kilobases; pT7, T7 RNA polymerase promoter; An, poly (A) tail.

509

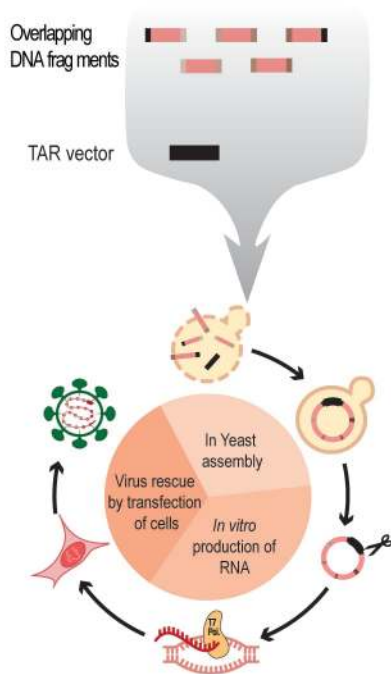
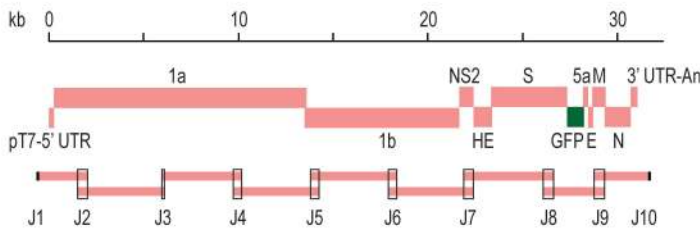
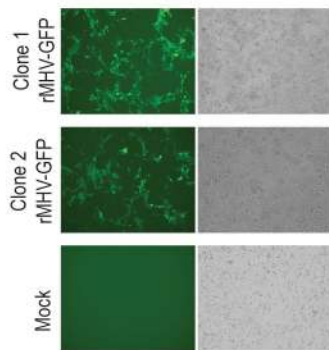
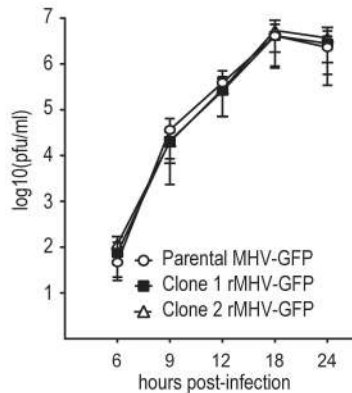
510 **Extended Data Figure 2**

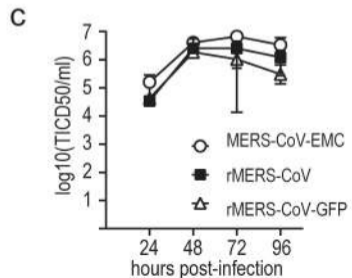
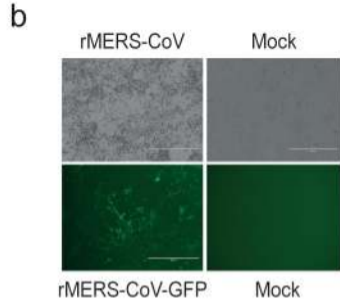
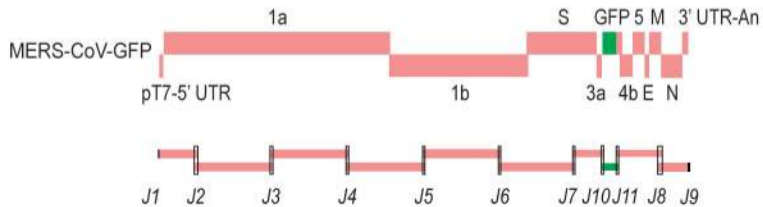
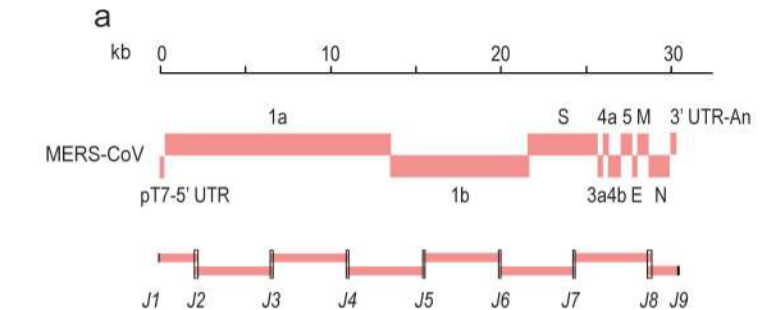
511 **a**, Six constructs were initially designed based on 3 different 5'-UTR regions. These regions
512 contain i) a modified sequence of the 5'-UTR region of the SARS-CoV-2 (5'- ATAUUAGG;
513 5'-terminal 8 nucleotides are shown, modified nucleotides underlined) were nucleotides 3-5
514 (UAA) of SARS-CoV-2 were changed to AUU to match the SARS-CoV nucleotides 3-5
515 (synthetic fragment 1.1 for constructs 1 and 4), ii) a SARS-CoV-2 5'-terminus with the first
516 124 nucleotides exchanged by the corresponding 5'-terminal sequence of SARS-CoV
517 (synthetic fragment 1.2; construct 2 and 5) and iii) the reported sequence of the SARS-CoV-2
518 (GISAID: EPI_ISL_402119) (synthetic fragment 1.3; constructs 3 and 6). After yeast
519 transformation, 10 colonies were randomly picked for each of the six constructs and all the
520 junctions bridging the overlapping fragments were verified by multiplex PCR. For each
521 construct, two clones (x.1 and x.2) were randomly selected and YAC DNAs were isolated (12
522 clones in total). RNAs were generated by *in vitro* transcription and electroporated together
523 with an mRNA encoding the SARS-CoV-2 N protein either into BHK-21 cells (12 clones) or
524 BHK-SARS-N cells (cells expressing the SARS-CoV N protein) (6 clones). Electroporated
525 cells were then co-cultivated with susceptible VeroE6 cells to rescue the recombinant viruses.
526 P.0 supernatants were collected at different time points after electroporation (from 2 dpe to 5

527 dpe) and transferred to VeroE6 cells to generate P.1 virus stocks, and in parallel to
528 demonstrate presence of infectious virus by plaque assay (virus clones that do not encode
529 GFP) or fluorescence microscopy (GFP-encoding virus clones). YAC, yeast artificial
530 chromosome; h.p.e, hours post-electroporation; d.p.e, days post-electroporation; CPE,
531 cytopathic effects; GFP, green fluorescent protein; pfu/ml, plaque forming units per millilitre.

532

533

a**b****c****d**



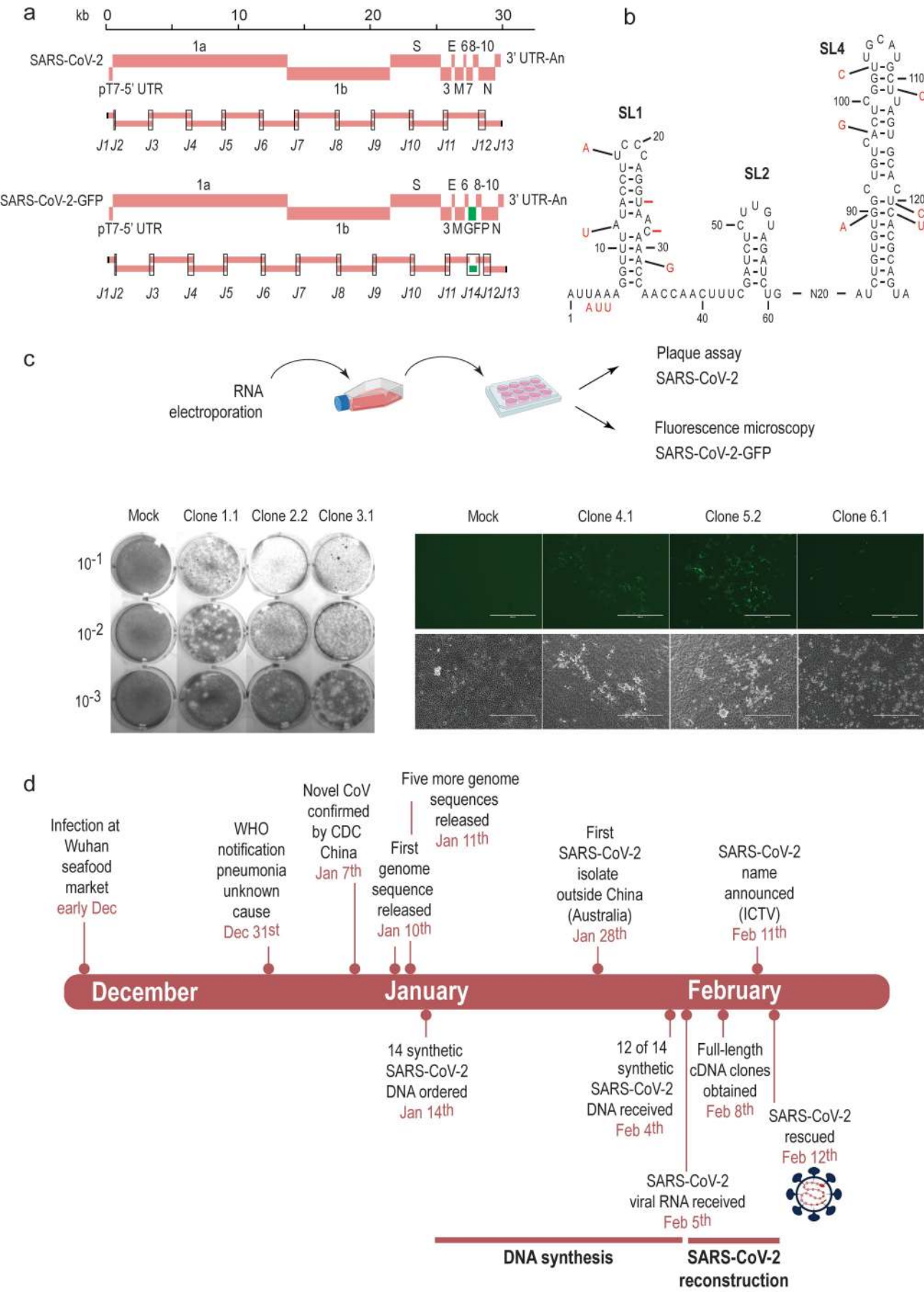


Table 1: RNA virus genomes cloned using the synthetic genomics platform

Virus	Family	RNA type	Size (kbp)	Template	Fragment generation	Number of assembled fragments*	Virus rescue
MHV-GFP	Coronaviridae	(+)RNA	31.9	Viral RNA (laboratory virus); DNA clone (vaccinia virus)	RT-PCR/PCR	9	yes
MERS-CoV	Coronaviridae	(+)RNA	30.1	DNA clone (BAC)	PCR	8	yes
MERS-CoV-GFP	Coronaviridae	(+)RNA	30.7	DNA clone (BAC) GFP plasmid DNA	PCR	10	yes
HCoV-229E	Coronaviridae	(+)RNA	27.3	Viral RNA (laboratory virus); DNA clone (vaccinia virus)	RT-PCR/PCR	13	in progress
HCoV-HKU1	Coronaviridae	(+)RNA	29.9	Synthetic DNA viral RNA (virus isolate)	PCR/RT-PCR	11	in progress
MERS-CoV-Riyadh-1734-2015	Coronaviridae	(+)RNA	(30)	Viral RNA (virus isolate)	RT-PCR	8	in progress
ZIKA virus	Flaviviridae	(+)RNA	10.8	Viral RNA (isolate)	RT-PCR	6	in progress
Human RSV-B	Paramyxoviridae	(-)RNA	15	Clinical sample	RT-PCR	4	in progress
SARS-CoV-2	Coronaviridae	(+)RNA	30	Synthetic DNA/viral RNA	plasmid DNA restriction/ RT-PCR	12	yes
SARS-CoV-2-GFP	Coronaviridae	(+)RNA	30.5	Synthetic DNA/viral RNA	plasmid DNA restriction/RT-PCR/PCR	14	yes

*excluding the TAR vector fragment